Novel Developmental Genes, *fruCD*, of *Myxococcus xanthus*: Involvement of a Cell Division Protein in Multicellular Development

Takuya Akiyama,[1] Sumiko Inouye,[2] and Teruya Komano[1]*

Department of Biology, Tokyo Metropolitan University, Minamiohsawa, Hachioji, Tokyo 192-0397, Japan,[1] and Department of Biochemistry, Robert Wood Johnson Medical School, Piscataway, New Jersey 08854[2]

Myxococcus xanthus **is a gram-negative soil bacterium that undergoes multicellular development upon nutrient starvation. In the present study, two novel developmental genes,** *fruC* **and** *fruD,* **of** *M. xanthus* **were identified and characterized. The FruD protein has significant amino acid sequence similarity to the DivIVA proteins of many bacteria including** *Bacillus subtilis.* **Vegetative cells of the** *fruD* **mutant exhibited a filamentous phenotype. The** *fruC* **and** *fruD* **mutants displayed similar delayed-development phenotypes. The formation of tightly aggregated mounds by** *fruC* **and** *fruD* **mutants was slower than that by the wild-type strain. Spore formation by the** *fruC* **and** *fruD* **mutants initiated after 30 h poststarvation, whereas wild-type** *M. xanthus* **initiated spore formation after 18 h. The** *fruCD* **genes were constitutively expressed as an operon during vegetative growth and development. S1 mapping revealed that transcription initiation sites of the** *fruCD* **operon were located 114 (P1) and 55 bp (P2) upstream of the** *fruC* **initiation codon. Only the P1 promoter was active during vegetative growth, while both the P1 and P2 promoters were active during development. The FruD protein was produced as a cytoplasmic protein and formed an oligomer during vegetative growth and development.**

Myxococcus xanthus, a gram-negative soil bacterium, is a model organism for studying mechanisms of multicellular morphogenesis and cell differentiation in prokaryotes, since the organism undergoes multicellular development upon nutrient starvation (7). During vegetative growth, *M. xanthus* cells grow in nutrient medium with a doubling time of approximately 4 h. Upon nutrient starvation on a solid surface, vegetative growth ceases and cells begin to gather into an aggregation center by gliding. Within 4 to 12 h poststarvation, the cells form mounds that are eventually converted into fruiting bodies. In the mounds, the motile, rod-shaped vegetative cells differentiate into nonmotile, refractile myxospores. Myxospores are resistant to sonication, heat, desiccation, and other stresses. When they are placed on a rich medium, they germinate to initiate vegetative growth.

Many developmentally defective *M. xanthus* mutants were isolated with Tn*V*, a Tn5-derived transposon carrying the *rep* region of pSC101 (11). Among 855 independent Tn*V* insertions, six were identified as developmental mutations. Three Tn*V* insertions, Ω221, Ω328, and Ω530, were located within a single gene, *lonD*, essential for the development of *M. xanthus*. The *lonD* gene is homologous to the *M. xanthus lonV* and *E. coli lon* genes and is identical to the *M. xanthus bsgA* gene (12, 31). One Tn*V* insertion, Ω786, was located within the upstream region of the *fruA* gene (23).

The *fruA* gene encodes a putative transcription factor essential for the development of *M. xanthus*. The amino acid sequence of the FruA protein contains a DNA-binding motif and has sequence similarity to response regulators of two-component His-Asp phosphorelay signal transduction systems (10, 23). The *fruA* gene was shown to play an important role in the C signal transduction pathway (10, 28). Genetic studies suggested that FruA may be activated by phosphorylation (10). Recently, we performed two-dimensional gel electrophoresis analysis to examine the effects of *csgA* and *fruA* mutations on the expression of *M. xanthus* developmental genes (16). While the expression of many developmental proteins was dependent on both *fruA* and *csgA*, several proteins including protein S and DofA were expressed in a *fruA*-dependent but *csgA*-independent manner. A model of the role of *fruA* in the C signal transduction pathway was proposed to explain these findings (10, 16). The gene encoding the DofA protein was cloned and characterized (14, 16). Regulation of *fruA* expression during vegetative growth and development was analyzed recently (15).

In this study, novel developmental genes *fruC* and *fruD* of *M. xanthus* were identified. The *fruC* and *fruD* genes are located 3 kb upstream of the *fruA* gene as an operon in the *M. xanthus* chromosome. The *fruC* and *fruD* mutants exhibited delayed-development phenotypes. The FruD protein exhibits significant amino acid sequence similarity to the DivIVA proteins of many bacteria.

MATERIALS AND METHODS

Microbial strains and plasmids. The bacterial strains used in this study were *M. xanthus* DZF1 *sglA1* (17), *Escherichia coli* DH5α *supE44* Δ*lacU169* (φ80 *lacZ*ΔM15) *hsdR17 recA1 gyrA96 thi-1 relA1* (2), and *E. coli* BL21(DE3) *dcm ompT hsdS gal* (29). *Saccharomyces cerevisiae* PJ69-4A *MAT***a** *trp1-901 leu2-3,112*

---

* Corresponding author. Mailing address: Department of Biology, Tokyo Metropolitan University, Minamiohsawa, Hachioji, Tokyo 192-0397, Japan. Phone: 81-426-77-2568. Fax: 81-426-77-2559. E-mail: komano-teruya@c.metro-u.ac.jp.
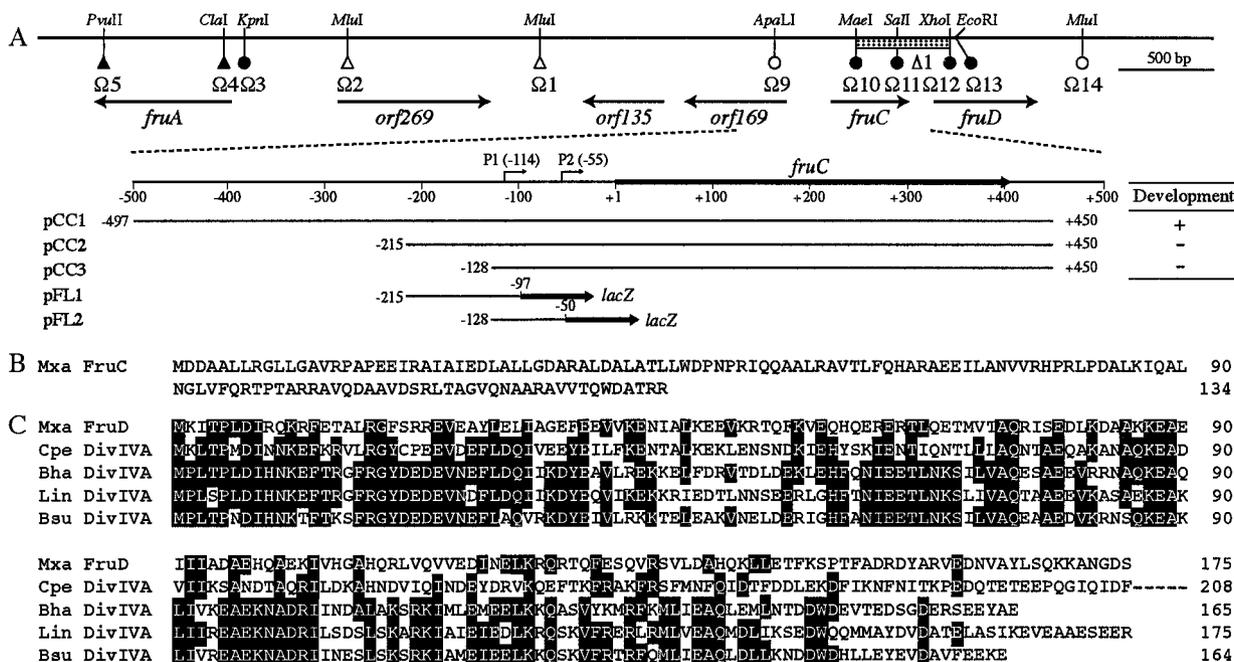
FIG. 1. (A) Gene organization of the *fruACD* region of *M. xanthus*. Top horizontal line, restriction map. Circles and triangles, locations of Km^r and Tc^r insertion mutations, respectively; open and filled symbols, insertional mutations promoting proficient development and those producing deficient development, respectively; stippled bar, location of Δ*fruCD1* mutation; arrows below the lines, *fruACD* genes and open reading frames deduced from the nucleotide sequence. The lower part of diagram shows an expanded view of the *fruC* region and the inserts of plasmids used for complementation experiment and promoter activity analysis. Bent arrows, P1 and P2 transcription initiation sites. The indicated DNA segments were synthesized by PCR and inserted into pTC1 or pSI1403attP. Nucleotide A of the *fruC* ATG initiation codon is indicated as +1. (B) FruC amino acid sequence deduced from the nucleotide sequence. Numbers on the right indicate residues from the N-terminal end. (C) Alignment of amino acid sequences of *M. xanthus* FruD and various bacterial DivIVA proteins. White lettering on a black background, identical amino acid residues in three or more sequences. Mxa, *M. xanthus*; Cpe, *C. perfringens*; Bha, *B. halodurans*; Lin, *L. innocua*; Bsu, *B. subtilis*.

ura3-52 his3-200 gal4 gal80 LYS2::GAL1-HIS3 GAL2-ADE2 met::GAL7-lacZ (19) was also used.

Plasmid vector pUC19 (34) was used for cloning. pET11 Km-GST (23) was used for overexpression of the *gst-fruD* gene. pSI1403attP (14) was used for construction of *lacZ* transcriptional fusions. pGADT7 and pGBKT7 (Clontech) were used for yeast two-hybrid system experiments. pMFA02 (23) is a pUC19 derivative carrying the *fruACD* region.

Growth conditions. *M. xanthus* cells were grown at 30°C in Casitone-yeast extract (CYE) medium (4) or on CYE agar (CYE medium containing 1.5% agar). Kanamycin sulfate (40 μg/ml) and oxytetracycline (6.25 μg/ml) were used for the selection of kanamycin-resistant (Km^r) and tetracycline-resistant (Tc^r) *M. xanthus* cells, respectively.

E. coli cells were grown at 37°C in Luria-Bertani medium (21). Ampicillin (100 μg/ml), kanamycin sulfate (50 μg/ml), or tetracycline (12.5 μg/ml) was used when required. Yeast cells were grown at 30°C in yeast-peptone-dextrose medium or synthetic dextrose (SD) medium (27).

Photographs of vegetative *M. xanthus* cells were taken through a phase-contrast microscope. To estimate average cell sizes, the lengths of more than 200 cells were measured.

Development and sporulation. Development of *M. xanthus* cells was induced on clone fruiting (CF) agar (13, 17). *M. xanthus* cells were grown to late log phase in CYE medium, washed once with TM buffer (10 mM Tris-HCl [pH 7.6], 8 mM MgSO₄), and resuspended in TM buffer at a density of 2 × 10^10 cells/ml. Aliquots (10 μl) of cell suspension were spotted on CF agar and incubated at 30°C. The spots were photographed through a dissecting microscope.

The number of spores was measured as described by Jain and Inouye (18). Developing cells of *M. xanthus* were scraped off the agar surface, suspended in TM buffer, and sonicated to disrupt vegetative cells. Sonication-resistant refractile spores were counted in a counting chamber under a microscope. For germination, sonication-resistant refractile spores were treated at 50°C for 2 h, spread on a CYE agar plate, and incubated at 30°C for 5 days. Colonies of vegetative cells were counted.

Recombinant-DNA techniques. Preparation of chromosomal and plasmid DNA, transformation, and other methods of DNA manipulation were performed as described elsewhere (26). pFC1 was constructed by inserting a 384-bp *Apa*LI-*Mae*I fragment containing the *fruC* promoter region into the *Hin*cII site of pUC19.

pTC1 was constructed by inserting a 1.4-kb *Eco*RI-*Bal*I fragment containing the Tc^r gene of pBR322 into the *Sal*I site of pMP001 (32), a pHSG399 derivative carrying the Mx8 *intP-attP* region. To construct plasmids for the complementation of the *fruC* mutation, three DNA fragments (Fig. 1A) were synthesized by PCR with appropriate primers, each containing an *Eco*RI site at the 5′ end, and inserted into the *Eco*RI site of pTC1, generating pCC1, pCC2, and pCC3. pCC series plasmids were integrated into the Mx8 *attB* site of the *M. xanthus fruC*::Km Ω10 chromosome to generate MxCC1, MxCC2, and MxCC3, respectively.

Insertion and deletion mutations in pMFA02 were made by digestion of pMFA02 DNA with appropriate restriction enzymes and ligation with a Km^r DNA fragment as described previously (23) (Fig. 1A). To construct *M. xanthus fruC*::Km Ω10, *fruD*::Km Ω12, and Δ*fruCD1* mutants, pMFA02 plasmid DNA was digested with *Mae*I, *Xho*I, and *Mae*I and *Xho*I, respectively, treated with an *E. coli* DNA polymerase I Klenow fragment, and then ligated with a 1.3-kb *Hin*dIII-*Sma*I fragment containing the Km^r gene of Tn5. Then the resultant plasmid DNAs were linearized with *Sca*I and introduced into *M. xanthus* DZF1 cells by electroporation (20). Replacement of the chromosome with Km^r insertions by double-homologous recombination was confirmed by Southern blot analysis (26).

RT-PCR. Total RNAs were extracted from vegetative cells and developing *M. xanthus* DZF1 cells at 6, 12, and 24 h poststarvation by the hot-phenol method (1) and treated with DNase I. The DNA primer 5′-CTTCACTTCCTCCTTGA GCG-3′ was hybridized with 1 μg of total RNA and treated with RAV-2 reverse transcriptase (RT) as specified by the manufacturer (Takara, Kyoto, Japan). Then, PCR was performed with DNA primers 5′-ATGAAAATCACTCCGCT CG-3′ and 5′-CGATGTTCTCCTTCACCACC-3′. The PCR product was analyzed by 2% agarose gel electrophoresis.

S1 nuclease mapping. The S1 nuclease mapping procedure was adapted from the method of Berk and Sharp (3). First, the 5′ ends of a 2,993-bp KpnI-MaeI fragment of pMFA02 DNA were labeled with [γ-^{32}P]ATP (3,000 Ci/mmol) by using Ready-To-Go T4 polynucleotide kinase (Amersham Pharmacia Biotech). Then the end-labeled fragment was digested with ApaLI. The 384-bp ApaLI-MaeI fragment was hybridized with 40 μg of total RNA from vegetative cells or developing cells at 6, 12, and 24 h poststarvation and treated with 40 U of S1 nuclease at 37°C for 30 min. Then, protected DNA fragments were analyzed on 6% polyacrylamide gels containing 8 M urea.

Promoter activity during vegetative growth and development. To separately assess in vivo promoter activity, the P1 promoter region (positions 97 to 215 upstream from the *fruC* initiation codon) and the P2 promoter region (positions 50 to 128 upstream from the *fruC* initiation codon) were synthesized by PCR with appropriate primers containing BamHI sites at their 5′ ends and then cloned into the BamHI site of pSI1403attP, giving pFL1 and pFL2, respectively (Fig. 1A). The orientations and sequences of inserted fragments were confirmed by DNA sequencing. pFL1 and pFL2 were integrated into the Mx8 attB site of the *M. xanthus* DZF1 chromosome to generate MxFL1 and MxFL2, respectively. β-Galactosidase specific activity was determined during vegetative growth and development as described previously (14). Units of β-galactosidase specific activity were nanomoles of o-nitrophenol produced per minute per milligram of protein.

Preparation of antiserum against FruD. To purify the FruD protein fused to glutathione S-transferase (GST), a gst-fruD fusion gene under the control of a T7 promoter was constructed. The *fruD* coding sequence was amplified by PCR and cloned into the NdeI-BamHI site of pET11 Km-GST (23) to generate pET11 Km-GST-*fruD*. E. coli BL21(DE3) cells harboring pET11 Km-GST-*fruD* were grown at 37°C in Luria-Bertani medium to an A_{620} of 0.5, then isopropyl-β-D-thiogalactopyranoside was added at a final concentration of 1 mM, and the culture was incubated for another 2 h. Induced cells from 200 ml of culture were harvested and suspended in phosphate-buffered saline (PBS; 137 mM NaCl, 8.1 mM Na$_2$HPO$_4$, 2.7 mM KCl, 1.5 mM KH$_2$PO$_4$ [pH 7.4]) at a density of 2 × 10^{10} cells/ml and then passed through a French pressure cell. The cell lysate was centrifuged at 10,000 × g at 4°C for 10 min. The pellet containing the GST-FruD inclusion body was denatured with 10 ml of PBS containing 3 M urea. The solubilized crude extract was refolded by dialysis against PBS. After dialysis, approximately 10% of the GST-FruD fusion protein was present in the soluble fraction. The soluble fraction containing the refolded GST-FruD fusion protein was loaded on a column of glutathione-Sepharose 4B (Amersham Pharmacia Biotech) equilibrated with PBS. The GST-FruD fusion protein was eluted with elution buffer (50 mM Tris-HCl [pH 8.0], 10 mM reduced glutathione). The purified GST-FruD fusion protein was used to immunize a rabbit.

Western blot analysis. Cell proteins were separated by sodium dodecyl sulfate–15% polyacrylamide gel electrophoresis (SDS–15% PAGE) and transferred to a nitrocellulose membrane. The membrane was blocked with PBS containing 3% skim milk, reacted with a 1,000-fold dilution of rabbit anti-GST-FruD antiserum, and then reacted with a 100-fold dilution of a biotin-labeled goat anti-rabbit immunoglobulin G antibody. The FruD protein was detected by immunoblotting with an ABC-POD (R) kit (Wako, Osaka, Japan).

FruD production during vegetative growth and development of *M. xanthus*. Vegetative cells and developing cells at 24 and 48 h poststarvation were dissolved in solubilizing buffer (2% SDS, 0.08 M Tris-HCl [pH 6.8], 10% glycerol, 0.1 M β-mercaptoethanol) and boiled for 5 min. Each sample was analyzed by SDS–15% PAGE. Then, the FruD protein was detected by Western blot analysis using anti-GST-FruD antiserum.

Subcellular fractionation of *M. xanthus* cells. *M. xanthus* vegetative cells were lysed by EDTA-lysozyme and fractionated to periplasm, cytoplasm, and total-membrane fractions as described previously (24). Each fraction was analyzed by SDS–15% PAGE. Then, localization of the FruD protein was determined by Western blot analysis using anti-GST-FruD antiserum.

Gel filtration chromatography. *M. xanthus* vegetative cells and developing cells at 6 h poststarvation were harvested, washed once with 0.1 M phosphate buffer (pH 6.8), resuspended in the same buffer, disrupted by sonication, and centrifuged at 100,000 × g for 30 min at 4°C. The supernatant fraction was subjected to TSK-Gel G2000 (Tosoh, Tokyo, Japan) gel filtration chromatography (0.1 M phosphate buffer [pH 6.8]; flow rate, 0.1 ml/min). Each fraction was analyzed by SDS–15% PAGE. The FruD protein was detected by Western blot analysis using anti-GST-FruD antiserum.

Yeast two-hybrid system. The *fruD* coding sequence was cloned into the NdeI-BamHI sites of pGADT7, containing the *GAL4* activation domain, and pGBKT7, containing the *GAL4* DNA-binding domain, to generate pGADT7-*fruD* and pGBKT7-*fruD*, respectively. Yeast transformation and two-hybrid selection were carried out with host strain PJ69-4A (19). β-Galactosidase activity from a reporter gene was assayed as described by Miller (21).

Nucleotide sequence accession number. The nucleotide sequence data for *fruCD* reported in this paper will appear in the DDBJ, EMBL, and GenBank nucleotide sequence databases under accession no. AB100269.

RESULTS

Two novel genes required for multicellular development in *M. xanthus*. Previously, we cloned and characterized the *fruA* gene, encoding a putative transcription factor required for multicellular development of *M. xanthus* (23). To investigate the possible presence of another developmental gene(s) in this region, the 4.4-kb *fruA* upstream region was sequenced (Fig. 1A). DNA sequence analysis revealed that five novel open reading frames exist in this region. *orf269* encodes a hypothetical protein conserved in several bacteria, and *orf169* encodes a DnaJ family protein. Six novel Km^r insertion mutations (Ω9 through Ω14) as well as one deletion mutation (Δ1) in this region were constructed in an E. coli plasmid. All seven mutations could be introduced into the *M. xanthus* chromosome by double-homologous recombination, indicating that no genes essential for vegetative growth are present in this region. *M. xanthus* cells carrying Km^r Ω10, Ω11, Ω12, and Ω13 insertions and the Δ1 deletion exhibited delayed-development phenotypes, while those carrying Km^r Ω9 and Ω14 insertions were development proficient. These results indicate that the two novel genes, designated *fruC* and *fruD*, are developmental genes (Fig. 1A). The *fruC* and *fruD* genes are located 3 and 3.5 kb upstream of the *fruA* gene, respectively, and are orientated oppositely to *fruA*.

To analyze the upstream regulatory region of the *fruC* gene, *fruC* segments with various lengths of upstream regions were integrated into the Mx8 attB site of the *M. xanthus* fruC::Km Ω10 chromosome, generating MxCC1 to MxCC3 (Fig. 1A). MxCC1 exhibited development similar to that of the wild type, whereas MxCC2 and MxCC3 exhibited delayed-development phenotypes. The results of complementation experiments indicate that a DNA segment up to 497 bp upstream of the *fruC* initiation codon is required for *fruC* expression.

Amino acid sequences of the *fruC* and *fruD* products. The *fruC* gene encodes a protein of 134 amino acids with a calculated molecular weight of 14,564 (Fig. 1B). No known proteins in databases have significant amino acid sequence similarity to the FruC protein. Computer analysis suggests that the FruC protein is a cytoplasmic protein. The *fruD* gene encodes a protein of 175 amino acids with a calculated molecular weight of 20,390 (Fig. 1C). The deduced amino acid sequence of the FruD protein has up to 45% identity with those of DivIVA proteins of many bacteria including *Geobacter metallireducens*, *Clostridium perfringens*, *Bacillus halodurans*, *Bacillus subtilis*, and *Listeria innocua*. Computer analysis suggests that the FruD protein is a cytoplasmic protein and that the central region of the FruD protein has an α-helical coiled-coil structure. *B. subtilis* DivIVA is also a cytoplasmic protein containing an α-helical coiled-coil structure (5, 9). As expected from the high G+C content of *M. xanthus* genomic DNA, *M. xanthus* genes have very high G+C content at the third-codon positions. The codon usages in the *fruC* and *fruD* genes were similar to those in other *M. xanthus* genes, and the G+C contents at the third-codon positions in the *fruC* and *fruD* genes were 91 and 90%, respectively.

Characterization of the *fruCD* mutants. *M. xanthus fruC*::Km Ω10, *fruD*::Km Ω12, and Δ*fruCD1* cells grew at the same rates as wild-type DZF1 cells in CYE medium. *B. subtilis divIVA* mutants produced filamentous cells, together with a few minicells (5, 8, 25). In *M. xanthus fruD*::Km and Δ*fruCD1* vegetative cultures, filamentous cells formed more frequently than in DZF1 cultures, while no minicells were found (data not shown). The average lengths of *M. xanthus fruD*::Km (11.9 ± 9.2 μm) and Δ*fruCD1* (11.0 ± 7.1 μm) vegetative cells were greater than that of DZF1 cells (6.3 ± 1.6 μm), while that of *fruC*::Km vegetative cells (5.6 ± 1.5 μm) was similar to that of DZF1 cells. These results suggest that the *M. xanthus fruD* mutant exhibits some impairment of cell division.

To examine the effects of *fruC* and *fruD* mutations on fruiting body formation, the processes of development in *M. xanthus fruC*::Km, *fruD*::Km, Δ*fruCD1*, and wild-type DZF1 strains were compared. Vegetative cells of each strain were concentrated, spotted on CF agar plates, and incubated at 30°C. The morphological changes during the development of each strain were photographed (Fig. 2A). The time courses for *fruC*, *fruD*, and Δ*fruCD1* mutant aggregation were slower than that measured for DZF1. Although the developmental time courses for the three mutants were slower than that for DZF1, the final fruiting body morphologies of the three mutants were similar to that of DZF1. When the *fruC*, *fruD*, and Δ*fruCD1* mutants were spotted on TM buffer-agar plates, similar delays in development were observed.

Sporulation of the *fruCD* mutants. To investigate the effects of the *fruCD* mutations on spore formation, the processes of sporulation for *M. xanthus fruC*::Km, *fruD*::Km, Δ*fruCD1*, and wild-type DZF1 strains were compared. Vegetative cells of each strain were concentrated and spotted on CF agar plates. Each spot was scraped off the agar surface during development, and the refractile spores were counted (Fig. 2B). In DZF1, spore formation started 18 h poststarvation. The number of DZF1 spores increased steadily until 30 h, when the number reached a maximal value. In contrast, the spore formation of the *fruC*, *fruD*, and Δ*fruCD1* mutants initiated similarly at 30 h poststarvation. After that time, the number of spores in the three mutants increased steadily until 48 h, when the number reached a maximal value. The rates of spore formation for the three mutants were similar to that for the wild type. The numbers of spores produced by the three mutants after 96 h were approximately 60% of the number produced by DZF1 (Fig. 2B). Over 75% of myxospores obtained from the fruiting bodies of *fruC*, *fruD*, and Δ*fruCD1* mutants and the wild-type DZF1 strain aged for 96 h germinated and formed colonies on a CYE plate after 5 days (data not shown).

Expression of the *fruCD* genes during vegetative growth and development of *M. xanthus*. The expression of the *fruCD* genes was examined by RT-PCR analysis (Fig. 3). Total RNAs were prepared from DZF1 vegetative cells and developing cells at 6, 12, and 24 h poststarvation and treated with RT. The synthesized cDNA was used as a template for PCR with primers within the *fruD* gene. The expected 133-bp RT-PCR product was amplified from total RNAs of every stage when treated by RT (Fig. 3, lanes 5 to 8), while it was not detectable in the absence of RT treatment (Fig. 3, lanes 1 to 4). Another PCR was performed with forward and reverse primers within the *fruC* and *fruD* genes, respectively. An RT-PCR product was
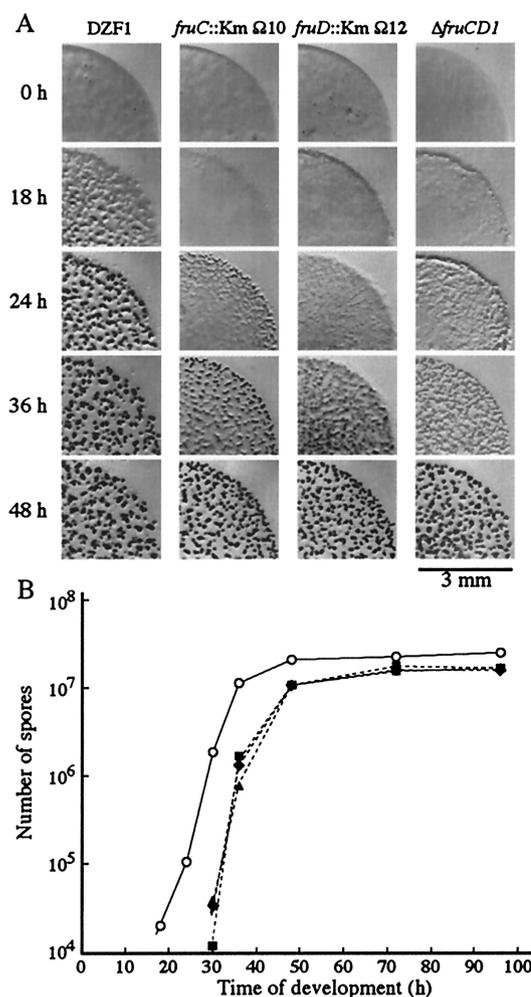

FIG. 2. (A) Morphogenesis during the development of *M. xanthus* DZF1 (wild type) and *fruC*::Km Ω10, *fruD*::Km Ω12, and Δ*fruCD1* mutants. Vegetative cells of each strain were spotted on CF agar plates. The spots were photographed through a dissecting microscope at the indicated times. (B) Sporulation of *M. xanthus* DZF1 (wild type) and *fruC*::Km Ω10, *fruD*::Km Ω12, and Δ*fruCD1* mutants. Vegetative cells (2×10^8) of each strain were spotted on CF agar. At the indicated times, the spots were scraped off the agar surface and sonicated. The refractile spores were counted in a counting chamber in triplicate. Open circles, DZF1 (wild type); solid squares, *fruC*::Km Ω10 mutant; solid triangles, *fruD*::Km Ω12 mutant; solid diamonds, Δ*fruCD1* mutant.

also amplified in this experiment (data not shown). These results indicate that the *fruCD* genes are expressed as an operon during vegetative growth and development.

Determination of the transcription initiation sites in the *fruCD* operon. To determine the transcription initiation site of the *fruCD* operon, S1 nuclease mapping analysis was performed with total RNAs prepared from vegetative cells and developing cells at 6, 12, and 24 h after starvation of *M. xanthus* DZF1. For RNAs from vegetative cells, one transcription initiation site (P1) was detected 114 bp upstream of the initiation codon of the *fruC* gene (Fig. 4A, lane V). For RNAs from developing cells, P1 and P2 transcription initiation sites were detected 114 and 55 bp, respectively, upstream of the initiation codon of the *fruC* gene (Fig. 4A and B, lanes D6, D12, and
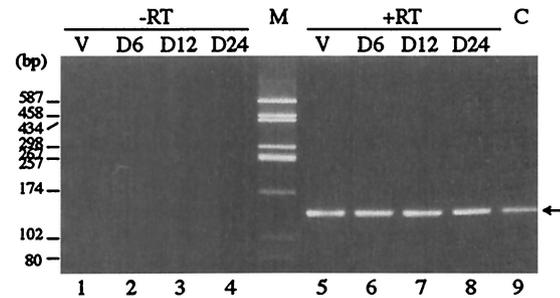
FIG. 3. Detection of the *fruD* transcript during vegetative growth and development of *M. xanthus*. Shown is RT-PCR analysis of *fruCD* expression in *M. xanthus*. Total RNAs prepared from vegetative cells (V) and developing cells at 6 (D6), 12 (D12), and 24 h (D24) post-starvation were treated with (+RT) or without (−RT) RT and subjected to PCR with appropriate primers. C, PCR product amplified from the *M. xanthus* DZF1 chromosome DNA; M, molecular weight standards, sizes of which are given on the left. Arrow, position of the 133-bp PCR product.

D24), while transcription from P1 decreased during development. These results indicate that the P1 promoter is active during vegetative growth and that activity decreases during development, while the P2 promoter is specific for development. From the sequence ladders shown in Fig. 4A and B, P1 and P2 transcription initiation sites mapped to the A and G residues, respectively, 114 and 55 bp upstream of the *fruC* initiation codon. Based on these results, the −35 and −10 regions for the two promoters of the *fruCD* operon are assigned as shown in Fig. 4C.

To demonstrate the in vitro activity of the P1 and P2 promoters, P1-*lacZ* and P2-*lacZ* transcriptional fusion genes were constructed and integrated into the Mx8 *attB* site of the *M.*

xanthus DZF1 chromosome, giving MxFL1 and MxFL2, respectively. MxFL1 exhibited 19 and 15 U of β-galactosidase activity during vegetative growth and 12 h poststarvation, respectively. MxFL2 exhibited 14 and 21 U of β-galactosidase activity during vegetative growth and 12 h poststarvation, respectively. These results indicate that P1 and P2 display promoter activity predominantly during vegetative growth and during development, respectively.

FruD protein production during vegetative growth and development. To examine FruD production during vegetative growth and development, total protein from vegetative cells and developing cells at 24 and 48 h after starvation of *M. xanthus* DZF1 and *fruC*::Km and *fruD*::Km mutants was separated by SDS-PAGE and subjected to Western blot analysis using anti-GST-FruD antiserum (Fig. 5A). In DZF1 cells, a protein band at 22 kDa was detected during vegetative growth and development; the density of the 22-kDa band decreased during development (Fig. 5A, lanes 1 to 3). The 22-kDa band was absent in the *fruD*::Km mutants during vegetative growth and development (Fig. 5A, lanes 7 to 9). These results indicate that the 22-kDa protein is the FruD protein. The estimated molecular mass of the FruD protein is in good agreement with the value of 20.4 kDa calculated from the DNA sequence. Since anti-GST-FruD antiserum was used in the present experiment, a protein band at 28 kDa is likely to be the GST protein of *M. xanthus*. FruD production in the *fruC*::Km mutant was similar to that in DZF1 (Fig. 5A, lanes 4 to 6), suggesting that the insertion mutation in the *fruC* gene does not affect FruD production.

Localization of the FruD protein. To examine the localization of the FruD protein, vegetative cells of *M. xanthus* DZF1 were disrupted and separated into periplasmic, cytoplasmic,
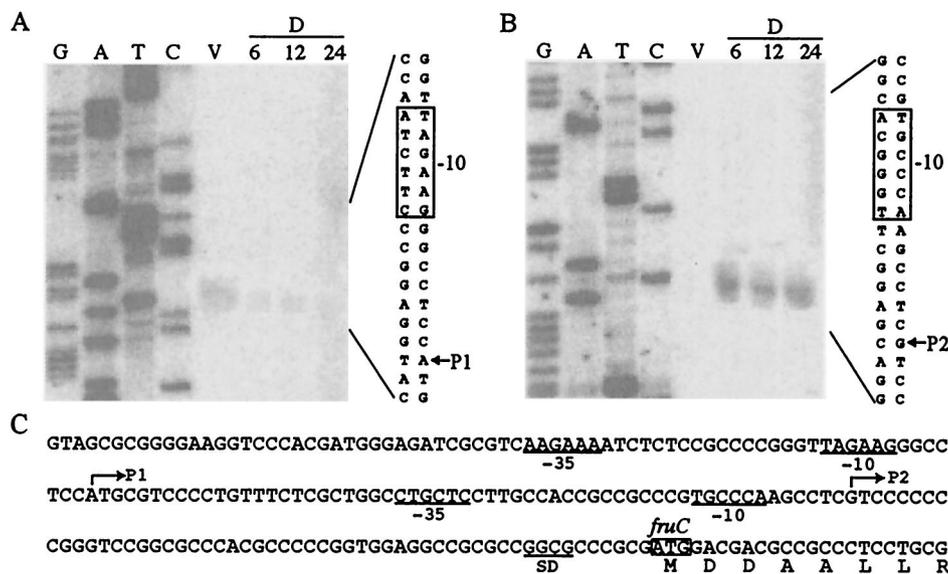

FIG. 4. (A and B) Transcription initiation sites of the *fruCD* mRNA. Total RNAs were prepared from *M. xanthus* DZF1 vegetative cells (V) and developing cells at 6, 12, and 24 h poststarvation and subjected to S1 mapping analysis. Arrows, positions of the S1-protected fragments; G, A, T, and C, sequence ladder generated by the dideoxy chain termination method with appropriate primers and with pFC1 DNA as the template. Panels A and B represent different locations of the gel for S1 mapping analysis. (C) Nucleotide sequence of the *fruCD* promoter region. Bent arrows, transcription initiation sites. The −35 and −10 regions and the putative Shine-Dalgarno sequence (SD) are underlined. The start codon of *fruC* is boxed. The N-terminal amino acid sequence of FruC is also indicated.
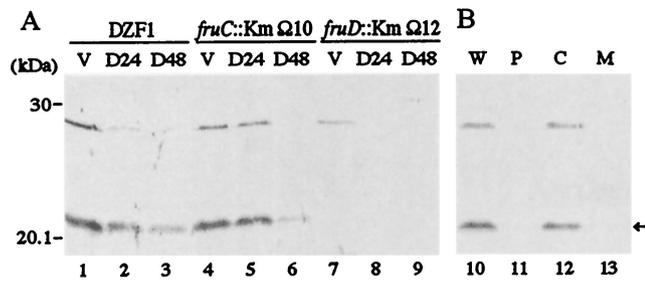
FIG. 5. (A) Western blot analysis of the *fruD* product. Total cell proteins from vegetative cells (V) and developing cells at 24 (D24) and 48 h (D48) after starvation of *M. xanthus* DZF1 (wild type) and *fruC*::Km Ω10 and *fruD*::Km Ω12 mutants were separated by SDS-PAGE. The FruD protein was detected by Western blot analysis using anti-GST-FruD antiserum. Molecular mass standards are given on the left. Arrow, position of the FruD protein. (B) Subcellular localization of the FruD protein. To determine the localization of the FruD protein, *M. xanthus* DZF1 cells from a vegetative culture were disrupted and separated to periplasmic, cytoplasmic, and total-membrane fractions. After SDS-PAGE, the FruD protein was detected by Western blot analysis using anti-GST-FruD antiserum. Molecular mass standards are given on the left. Arrow, position of the FruD protein. Lanes: W, whole cell; P, periplasm; C, cytoplasm; M, total membrane.

and total-membrane fractions. After SDS-PAGE of each fraction, the FruD protein was detected by Western blot analysis using anti-GST-FruD antiserum (Fig. 5B). The FruD protein was detected as the 22-kDa band only in the cytoplasmic fraction (Fig. 5B, lane 12). These results indicate that the *fruD* gene is expressed as a cytoplasmic protein. The localization of the FruD protein in the cytoplasm is consistent with the prediction of computer analysis described above.

Oligomer formation of the FruD protein. Oligomer formation of the *B. subtilis* DivIVA protein has been reported (22). To examine whether the FruD protein exists as a monomer or an oligomer under native conditions, soluble fractions from *M. xanthus* vegetative cells and developing cells at 6 h poststarvation were subjected to gel filtration chromatography. After TSK-Gel G2000 gel filtration chromatography, each eluate fraction was analyzed by SDS-PAGE followed by Western blot analysis using anti-GST-FruD antiserum (Fig. 6A). The FruD proteins from both vegetative cells and developing cells were

eluted at positions corresponding to an oligomer. From the elution patterns of molecular weight markers, the molecular mass of the native FruD oligomer was estimated to be approximately 100 kDa. Since the monomer size of the FruD protein was estimated to be 20.4 kDa as described above, it is likely that the FruD protein exists as an oligomer in vegetative and developing cells of *M. xanthus*.

The yeast two-hybrid system was used to ascertain the FruD-FruD interaction. The *fruD* gene was cloned into two-hybrid system vectors pGADT7 and pGBDT7. Yeast cells containing pGADT7-*fruD* and pGBKT7-*fruD* formed colonies on SD medium lacking tryptophan, leucine, histidine, and adenine at 30°C after 1 week (Fig. 6B), indicative of a FruD-FruD interaction. A similar result was obtained when the FruD-FruD interaction was measured by a β-galactosidase assay (Fig. 6B). These findings are consistent with the results of gel filtration chromatography demonstrating that the FruD protein exists as an oligomer.

DISCUSSION

In this study, two novel developmental genes, *fruC* and *fruD*, of *M. xanthus* were analyzed. The *fruCD* genes were constitutively expressed as an operon during vegetative growth and development. From S1 nuclease mapping analysis, two distinct promoters (P1 and P2) for the *fruCD* operon were identified. The P1 promoter was active during vegetative growth and became weaker during development, while the P2 promoter was specific for development, suggesting that *fruCD* transcription is differently regulated during vegetative growth and development of *M. xanthus*. In vivo activity of the P1 and P2 promoters was demonstrated by P1-*lacZ* and P2-*lacZ* transcriptional fusions, although their β-galactosidase activity was not so high. Complementation experiments involving the *fruC* mutation revealed that a *fruC* region further upstream is required for *fruCD* expression. These results suggest the presence of a *cis* regulatory element(s) at the region of *fruC* promoters further upstream, since such regulatory elements are reportedly in many *M. xanthus* genes, including *dofA* and *fruA* (14, 15). Lack of the regulatory element(s) may explain the observed β-galactosidase activity from the P2 promoter during vegetative growth.
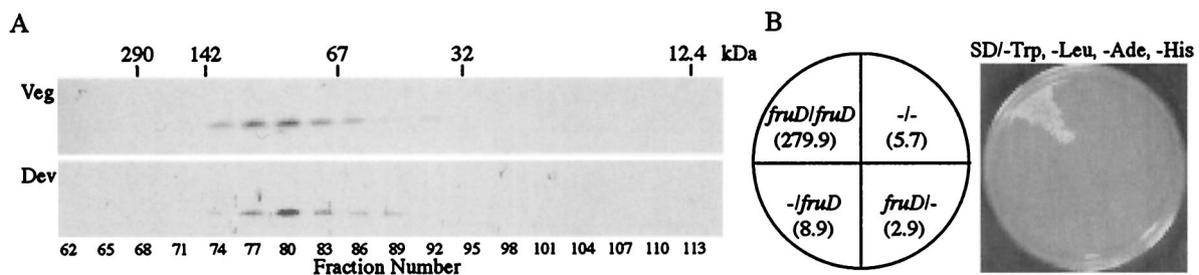

FIG. 6. Oligomer formation of the FruD protein. (A) Gel filtration chromatography of the FruD protein. Soluble proteins were prepared from *M. xanthus* vegetative cells (Veg) and developing cells (Dev) at 6 h poststarvation and subjected to TSK-Gel G2000 gel filtration chromatography. After SDS-PAGE of eluate fractions, the FruD protein was detected by Western blot analysis using anti-GST-FruD antiserum. The elution positions of molecular mass standards are indicated at the top (290 kDa, glutamate dehydrogenase; 142 kDa, lactose dehydrogenase; 67 kDa, enolase; 32 kDa, adenylate kinase; 12.4 kDa, cytochrome *c*). (B) FruD-FruD interaction in the yeast two-hybrid system. *S. cerevisiae* PJ69-4A cells containing pGADT7 and pGBDT7 with or without the *fruD* gene were grown at 30°C on SD medium lacking tryptophan, leucine, histidine, and adenine. The β-galactosidase activity (units) of each transformant is shown in parentheses.

Several *M. xanthus* genes which are expressed by two distinct promoters have been reported. The *M. xanthus sigD* gene, encoding a stationary-phase sigma factor, has two distinct promoters (33). Expression of the *sigD* gene is differently regulated by the two promoters during vegetative growth and development: the downstream of promoter is specific for development. The Δ*sigD* mutant exhibited growth defects during the late log phase and stationary phase, with reduced cell viability. The deletion mutant displayed a delayed-development phenotype, yielding fewer spores than the wild type.

The FruD protein displays significant amino acid sequence similarity to the DivIVA proteins of many bacteria such as *B. subtilis*. The DivIVA protein is known to be a functional homologue of the *E. coli* MinE protein, although the amino acid sequences of the DivIVA proteins exhibit no similarity to that of the MinE protein (5, 8). The *E. coli* MinE protein determines the division site, which is at the middle of the cell, by controlling the topological specificity of MinCD division inhibitors. The *B. subtilis* DivIVA protein also sequesters MinCD division inhibitors at the cell poles (5, 8). Vegetative cells of the *M. xanthus fruD* mutant exhibited a filamentous phenotype similarly to that the *B. subtilis divIVA* mutant. Therefore, it is likely that the *M. xanthus* FruD protein is involved in cell division, although the exact function of the FruD protein in cell division is not clear.

A second function of the *B. subtilis* DivIVA protein in sporulation has been reported (30). In sporulating cells, the *B. subtilis* DivIVA protein participates in chromosome segregation. It interacts with the chromosome segregation machinery to help position the *oriC* region of the chromosome at the cell pole in preparation for asymmetric division. The developmental processes of *M. xanthus* differ from those of *B. subtilis* in many points. Upon nutritional starvation on a solid surface, *M. xanthus* cells aggregate to form mounds, within which cells are converted into myxospores. In contrast, upon nutritional starvation in a liquid, *B. subtilis* cells undergo asymmetric cell division leading to the formation of endospores. It is of great interest that a cell division gene may also participate in bacterial development in both *M. xanthus* and *B. subtilis.*

The *fruC*, *fruD*, and Δ*fruCD* mutants displayed similar delayed-development phenotypes. The start of spore formation in the three mutants was delayed by 12 h in comparison to that for the wild type, while the rates of spore formation in *fruC* and *fruD* mutants were similar to that in the wild type. These results suggest that the FruC and FruD proteins may play similar roles at an aggregation stage during development in *M. xanthus*. It is possible that the retardation of spore formation in *fruC* and *fruD* mutants is due to delayed aggregation. The recently described genes *espAB* may control the timing of spore formation in coordination with aggregation (6). Sporulation of the *espA* mutant occurred faster than that of the wild type, while the *espB* mutant sporulated more slowly than the wild type. The EspA protein has significant amino acid sequence similarity to a sensor protein of a two-component signal transduction system and is considered to function as an inhibitor that delays sporulation until developmental aggregation is complete, while the EspB protein may antagonize EspA function. The phenotype of the *espB* mutant exhibits some similarity to those of the *fruC*, *fruD*, and Δ*fruCD1* mutants.

Homooligomer formation of the *B. subtilis* DivIVA protein

has been reported (22). Since some *B. subtilis* DivIVA mutants failed to form normal DivIVA oligomers, DivIVA oligomer formation may be crucial for its activity. In the present study, the size of the native form of the *M. xanthus* FruD protein was estimated to be approximately 100 kDa. If one postulates that the FruD protein forms homooligomers, the number of FruD monomers may be four or five. This value is significantly lower than the reported value of 10 to 12 for the *B. subtilis* DivIVA oligomer. Further studies are necessary to understand the function of the FruC and FruD proteins in the development of *M. xanthus*.

REFERENCES

1. **Aiba, H., S. Adhya, and B. de Crombrugghe.** 1981. Evidence for two functional *gal* promoters in intact *Escherichia coli* cells. J. Biol. Chem. **256:**11905–11910.
2. **Ausubel, F., R. Brent, R. E. Kingston, D. D. Moore, J. G. Seidman, J. A. Smith, and K. Struhl (ed.).** 1988. Current protocols in molecular biology. John Wiley & Sons, New York, N.Y.
3. **Berk, A. J., and P. A. Sharp.** 1977. Sizing and mapping of early adenovirus mRNAs by gel electrophoresis of S1 endonuclease-digested hybrids. Cell **12:**721–732.
4. **Campos, J. M., J. Geisselsoder, and D. R. Zusman.** 1978. Isolation of bacteriophage Mx4, a generalized transducing phage for *Myxococcus xanthus.* J. Mol. Biol. **119:**167–178.
5. **Cha, J.-H., and G. C. Stewart.** 1997. The DivIVA minicell locus of *Bacillus subtilis*. J. Bacteriol. **179:**1671–1683.
6. **Cho, K., and D. R. Zusman.** 1999. Sporulation timing in *Myxococcus xanthus* is controlled by the *espAB* locus. Mol. Microbiol. **34:**714–725.
7. **Dworkin, M.** 1996. Recent advances in the social and developmental biology of the myxobacteria. Microbiol. Rev. **60:**70–102.
8. **Edwards, D. H., and J. Errington.** 1997. The *Bacillus subtilis* DivIVA protein targets to the division septum and controls the site specificity of cell division. Mol. Microbiol. **24:**905–915.
9. **Edwards, D. H., H. B. Thomaides, and J. Errington.** 2000. Promiscuous targeting of *Bacillus subtilis* cell division protein DivIVA to division sites in *Escherichia coli* and fission yeast. EMBO J. **19:**2719–2727.
10. **Ellehauge, E., M. Norregaard-Madsen, and L. Søgaard-Andersen.** 1998. The FruA signal transduction protein provides a checkpoint for the temporal coordination of intercellular signals in *Myxococcus xanthus* development. Mol. Microbiol. **30:**807–817.
11. **Furuichi, T., M. Inouye, and S. Inouye.** 1985. Novel one-step cloning vector with a transposable element: application to the *Myxococcus xanthus* genome. J. Bacteriol. **164:**270–275.
12. **Gill, R. E., M. Karlok, and D. Benton.** 1993. *Myxococcus xanthus* encodes an ATP-dependent protease which is required for developmental gene transcription and intercellular signaling. J. Bacteriol. **175:**4538–4544.
13. **Hagen, D. C., A. P. Bretscher, and D. Kaiser.** 1978. Synergism between morphogenetic mutants of *Myxococcus xanthus*. Dev. Biol. **64:**284–296.
14. **Horiuchi, T., T. Akiyama, S. Inouye, and T. Komano.** 2002. Analysis of *dofA*, a *fruA*-dependent developmental gene, and its homologue, *dofB*, in *Myxococcus xanthus*. J. Bacteriol. **184:**6803–6810.
15. **Horiuchi, T., T. Akiyama, S. Inouye, and T. Komano.** Regulation of *fruA* expression during vegetative growth and development of *Myxococcus xanthus*. J. Mol. Microbiol. Biotechnol., in press.
16. **Horiuchi, T., M. Taoka, T. Isobe, T. Komano, and S. Inouye.** 2002. Role of *fruA* and *csgA* genes in gene expression during development of *Myxococcus xanthus*: analysis by two-dimensional gel electrophoresis. J. Biol. Chem. **277:**26753–26760.
17. **Inouye, M., S. Inouye, and D. R. Zusman.** 1979. Gene expression during development of *Myxococcus xanthus*: pattern of protein synthesis. Dev. Biol. **68:**579–591.
18. **Jain, R., and S. Inouye.** 1998. Inhibition of development of *Myxococcus xanthus* by eukaryotic protein kinase inhibitors. J. Bacteriol. **180:**6544–6550.
19. **James, P., J. Halladay, and E. A. Craig.** 1996. Genomic libraries and a host strain designed for highly efficient two-hybrid selection in yeast. Genetics **144:**1425–1436.
20. **Kashefi, K., and P. L. Hartzell.** 1995. Genetic suppression and phenotypic masking of a *Myxococcus xanthus frzF* defect. Mol. Microbiol. **15:**483–494.
21. **Miller, J. H.** 1972. Experiments in molecular genetics. Cold Spring Harbor Laboratory, Cold Spring Harbor, N.Y.

22. **Muchova, K., E. Kutejova, D. J. Scott, J. A. Brannigan, R. J. Lewis, A. J. Wilkinson, and I. Barak.** 2002. Oligomerization of the *Bacillus subtilis* division protein DivIVA. Microbiology **148:**807–813.

23. **Ogawa, M., S. Fujitani, X. Mao, S. Inouye, and T. Komano.** 1996. FruA, a putative transcription factor essential for the development of *Myxococcus xanthus*. Mol. Microbiol. **22:**757–767.

24. **Orndorff, P. E., and M. Dworkin.** 1980. Separation and properties of the cytoplasmic and outer membranes of vegetative cells of *Myxococcus xanthus*. J. Bacteriol. **141:**914–927.

25. **Reeve, J. N., N. H. Mendelson, S. I. Coyne, L. L. Hallock, and R. M. Cole.** 1973. Minicells of *Bacillus subtilis*. J. Bacteriol. **114:**860–873.

26. **Sambrook, J., E. F. Fritsch, and T. Maniatis.** 1989. Molecular cloning: a laboratory manual, 2nd ed. Cold Spring Harbor Laboratory Press, Cold Spring Harbor, N.Y.

27. **Sherman, F.** 1991. Getting started with yeast. Methods Enzymol. **194:**3–21.

28. **Søgaard-Andersen, L., F. J. Slack, H. Kimsey, and D. Kaiser.** 1996. Intercellular C-signaling in *Myxococcus xanthus* involves a branched signal transduction pathway. Genes Dev. **15:**740–754.

29. **Studier, F. W., and B. A. Moffatt.** 1986. Use of bacteriophage T7 RNA polymerase to direct selective high-level expression of cloned genes. J. Mol. Biol. **189:**113–130.

30. **Thomaides, H. B., M. Freeman, M. El Karoui, and J. Errington.** 2001. Division site selection protein DivIVA of *Bacillus subtilis* has a second distinct function in chromosome segregation during sporulation. Genes Dev. **15:**1662–1673.

31. **Tojo, N., S. Inouye, and T. Komano.** 1993. The *lonD* gene is homologous to the *lon* gene encoding an ATP-dependent protease and is essential for the development of *Myxococcus xanthus*. J. Bacteriol. **175:**4545–4549.

32. **Tojo, N., K. Sanmiya, H. Sugawara, S. Inouye, and T. Komano.** 1996. Integration of bacteriophage Mx8 into the *Myxococcus xanthus* chromosome causes a structural alteration at the C-terminal region of the IntP protein. J. Bacteriol. **178:**4004–4011.

33. **Ueki, T., and S. Inouye.** 1998. A new sigma factor, SigD, essential for stationary phase is also required for multicellular differentiation in *Myxococcus xanthus*. Genes Cells **3:**371–385.

34. **Yanisch-Perron, C., J. Vieira, and J. Messing.** 1985. Improved M13 phage cloning vectors and host strains: nucleotide sequences of M13mp18 and pUC19 vectors. Gene **33:**103–119.